HHS Public Access

Author manuscript

Chemistry. Author manuscript; available in PMC 2023 April 27.

Published in final edited form as:

Chemistry. 2022 April 27; 28(24): e202104430. doi:10.1002/chem.202104430.

Metalloimmunotherapy with Rhodium and Ruthenium Complexes: Targeting Tumor-Associated Macrophages

Dr. Nicholas Toupin[a], **Mackenzie K. Herroon**[b], **Randolph P. Thummel**[c] **[Prof.]**, **Claudia Turro**[d] **[Prof.]**, **Izabela Podgorski**[b,f] **[Prof.]**, **Heather Gibson**[e,f] **[Prof.]**, **Jeremy J. Kodanko**[a,f] **[Prof.]**

[a]Department of Chemistry, Wayne State University, 5101 Cass Ave, Detroit, MI 48202 (USA)

[b]Department of Pharmacology, School of Medicine, Wayne State University, Detroit, MI 48201 (USA)

[c]Department of Chemistry, University of Houston, Houston, Texas 77204-5003 (USA)

[d]Department of Chemistry and Biochemistry, The Ohio State University, Columbus, Ohio 43210 (USA)

[e]Department of Oncology, Wayne State University, Detroit, MI 48201 (USA)

[f]Karmanos Cancer Institute, Detroit, Michigan 48201 (USA)

Abstract

Tumor associated macrophages (TAMs) suppress the cancer immune response and are a key target for immunotherapy. The effects of ruthenium and rhodium complexes on TAMs have not been well characterized. To address this gap in the field, a panel of 22 dirhodium and ruthenium complexes were screened against three subtypes of macrophages, triple-negative breast cancer and normal breast tissue cells. Experiments were carried out in 2D and biomimetic 3D co-culture experiments with and without irradiation with blue light. Leads were identified with cell-type-specific toxicity toward macrophage subtypes, cancer cells, or both. Experiments with 3D spheroids revealed complexes that sensitized the tumor models to the chemotherapeutic doxorubicin. Cell surface exposure of calreticulin, a known facilitator of immunogenic cell death (ICD), was increased upon treatment, along with a concomitant reduction in the M2-subtype classifier arginase. Our findings lay a strong foundation for the future development of ruthenium- and rhodium-based chemotherapies targeting TAMs.

Graphical Abstract

jkodanko@wayne.edu .

Conflict of Interest

The authors declare no conflict of interest.

Supporting information for this article is available on the WWW under https://doi.org/10.1002/chem.202104430

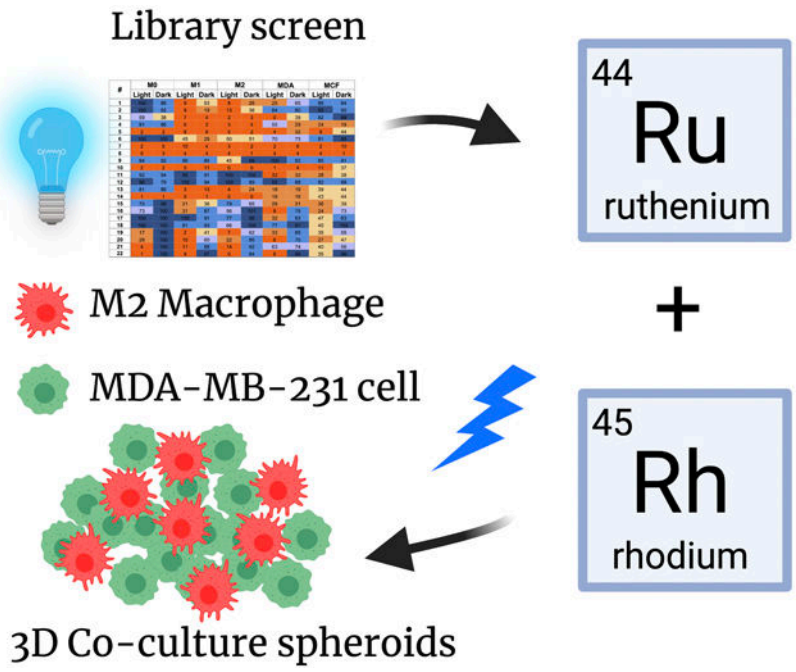

Keywords

antitumor agents; immunotherapy; macrophage; rhodium; ruthenium; transition metals

Introduction

The human immune system involves a complex interplay between chemical signals and biological responses. Macrophages play an essential role in humans and the immune response, including maintenance of tissue homeostasis through breakdown of senescent cells, mediation of the inflammatory immune response, wound healing, and foreign pathogen detection.[1] In addition to their essential roles in normal health, macrophages also fuel the progression of human diseases, including those caused by chronic inflammation, such as atherosclerosis[2] and cancer.[3]

Macrophages display a high degree of cellular plasticity and are able to make drastic changes in their behavior depending on their environment.[4] The classical definition for macrophage subtyping holds that M0 or undifferentiated macrophages can differentiate into two forms; either pro-inflammatory (M1) or anti-inflammatory (M2) macrophages. M1 macrophages are responsible for pathogen detection, triggering inflammation via release of pro-inflammatory cytokines, and cytotoxicity through the production of reactive oxygen and nitrogen species.[4] M2 macrophages, on the other hand, are immuno-suppressive and act to reduce inflammation caused from M1 macrophages.[4–5] The balance between M1 and M2 polarization affects not only the local inflammatory milieu, but also influences adaptive immune priming.

Cancer is the second leading cause of death in the US, and progresses in large part due to the inability of the host immune system to eliminate transformed cells and differentiate between cancer and its own healthy cells.[6] The most aggressive cancer cells secrete chemical signals, also known as chemokines, to recruit M0 macrophages into tumor tissue.[7] Upon accumulation at the tumor site, M0 macrophages further differentiate to either the M1 or M2 subtype, which are known collectively as tumor associated macrophages (TAMs). Tumors with high numbers of M2 TAMs are associated with poor prognoses and more severe outcomes.[8] Furthermore, M2 TAMs display an immunosuppressive capacity by expressing programmed death ligands 1 and 2 (PD-L1/2) which in turn bind to the PD-1 receptor on killer T-cells, suppressing their capacity to kill tumor cells.[9] M2 TAMs also downregulate levels of pro-inflammatory M1 macrophages through mediation of polyamine signaling and metabolism, reducing pro-immune inflammation at the tumor site.[5]

The first immunotherapy for the treatment of cancer began in the 1980's with the FDA approval of the cytokine interferon alpha 2 (IFN-α2).[10] More recently, immune checkpoint therapies targeting the CTLA-4 and PD-1 pathways have spawned a new era and interest in harnessing the immune system to fight cancer.[11] Likewise, due to their outsized role in tumor progression, macrophages have also been identified as prime targets for anti-tumor immunotherapies.[12] There are two main strategies for targeting macrophages. The first is macrophage repolarization or switching the TAM phenotype from the immunosuppressive M2 state to the anti-tumor M1 state through chemical signaling.[13] The second approach involves macrophage depletion, or simply macrophage-specific toxicity. Common treatment modalities for macrophage depletion include nanoparticles[14] and photosensitizing agents.[15] Macrophage-specific photodynamic therapy (PDT), represents an exciting opportunity for anti-tumor activity.[15] PDT is a photochemical process, which unlike macrophage depletion, allows for spatiotemporal control over cell killing.

Historically, metal complexes have played a major role in cancer therapy. Cisplatin, and its derivatives, are currently used to treat roughly 50 % of human cancers. Unfortunately, platinum agents show low specificity towards cancer versus normal cells, leading to harrowing side effects in patients. Inspired by the success of platinum drugs and the need to discover more selective and less toxic metal-based compounds, recent efforts to develop new anti-cancer therapeutics have focused on other late transition metals, including ruthenium[16] and rhodium.[17] Ruthenium complexes have many attractive properties for PDT and photochemotherapy (PCT)[18] due to their high dark-to-light ratios for cancer cell death.[19] In addition, dirhodium paddlewheel complexes have been known for over 40 years to show promising activity in cancer cells, including cytostatic behavior[20] and more recently photo-induced damage to DNA.[21,17a] Altogether hundreds of research articles have been published concerning the evaluation synthesis of Ru and Rh complexes as anti-cancer agents.[22] These compounds have undergone rigorous testing in a myriad of different in vitro and in vivo models of human cancers, including breast, prostate, lung, colon, skin, bladder and brain.[22a,b] Several ruthenium-based drugs have entered human clinical trials.[23] Given the large role immune cells and signaling play in cancer progression and survival, the effects of metal compounds on immune cells, including macrophages, are still fragmentary.[22c] This is especially true for Ru and Rh complexes whose effects on macrophages has been reported minimally.[24]

Herein we describe the evaluation of a library of ruthenium- and rhodium-based complexes against M0, M1, and M2 murine macrophages. To provide points of comparison, this library was also screened against the human triple-negative breast cancer (TNBC) cell line MDA-MB-231 and the normal human breast epithelial line MCF-10 A. After screening the full library, in the dark and under visible light irradiation to uncover compounds with PDT/PCT effects, rich structure-activity relationships were revealed, and leads were identified. From EC_{50} determinations in 2D cell culture experiments, we discovered complexes with specific toxicity toward macrophages versus cancer cells and normal cells, as well as compounds that are specific for killing immunosuppressive M2 macrophages versus non-polarized M0 macrophages or pro-inflammatory M1 cells. Furthermore, several compounds in our series showed high selectivity for killing cells under light versus dark conditions. A subset of the most promising compounds from 2D studies was carried into 3D cell co-culture experiments, where spheroids containing macrophages and TNBC cells were used to mimic the in vivo tumor microenvironment, modeling the signaling between TAMs and cancer cells that modulates the phenotype of these populations. Key functional markers were probed to identify the transition between M1 and M2 macrophages, as well as tumor cell surface calreticulin exposure, a classifier of immunogenic cell death (ICD) that can lead to long-lasting anti-tumor immunity. These studies revealed that Ru and Rh metal-based agents can kill M2 macrophages in 3D culture and sensitize tumor spheroids to the cancer drug doxorubicin, an inducer of ICD. Furthermore, imaging experiments confirmed that the lead metal complexes increase calreticulin translocation to the cancer cell surface. This study opens new avenues for metalloimmunotherapy with rhodium and ruthenium compounds.

Results and Discussion

Compounds **1**–**22** (Figure 1) were selected for this study because they represent a diverse group of dinuclear rhodium and mononuclear ruthenium complexes. A wide net was cast because structure activity relationships (SAR) are notoriously difficult to predict for metal complexes. Rh_2(II,II) paddlewheel complexes **1**,[25] **2**–**3**,[26] **4**,[27] and **5**[28] are derived from bidentate or tridentate polypyridyl ligands. Compounds **6**[29] and **7**[30] are mononuclear Ru(II) complexes containing the ligand dqpy (2,6-di(quinolin-2-yl)pyridine), which supports photosensitization and/or photorelease chemistry,[31] depending on the nature of the other mono- or bidentate ligands. Complex **8**[31] carries the tridentate ligand tpy (2,2′:6′,2′′-terpyridine) and the bidentate ligand 2,2,6,6-tetramethylheptane-3,5-dione. However, unlike complexes containing the Ru(dqpy) fragment, which are largely unexplored in biological applications, there are many examples of those with the Ru(tpy) unit that show photosensitization and/or photorelease properties in vitro and in vivo.[32] Analogs **9**,[33] **10**,[34] **11**,[35] **12**,[36] and **13**–**15**[37] all contain the fragment $Ru(bpy)_2$, a molecular scaffold found in many bioactive Ru(II) complexes that show photorelease, photosensitization and, in many cases, luminescence.[38] Compounds **16**[39] and **17**–**19**[40] are photoactive Ru(II) complexes that release monodentate nitriles, complex **19** induces apoptosis in MDA-MB-231 cells upon irradiation with blue light[41] and **20**[42] is a phosphine-containing complex containing the related fragment $Ru(phen)_2$ (phen = 1,10-phenanthroline). Compound **21**[43] is a homoleptic Ru(II) complex coordinated by the tridentate ligand pydppn (3-(pyridin-2-yl)benzo[*i*]dipyrido[3,2-*a*:2′,3′-

c]phenazine), which carries an extended π-system that facilitates photochemical protein-DNA crosslinking in cells.[44] Finally compound **22**[45] contains the Ru(tpy) fragment and the sterically encumbered ligand Me_2dppn (3,6-dimethylbenzo[*i*]dipyrido[3,2-*a*:2′,3′-*c*]phenazine), which facilitates photochemical release of monodentate pyridine ligands bound to ruthenium, as well as generation of $^1O_2$ for PCT/PDT dual-action behavior.[46]

General compound screen

Compounds **1**–**22** were screened at a single concentration in cell viability assays against a panel of five different cell types; M0, M1, and M2 murine macrophages, MDA-MB-231 triple-negative breast cancer cells, and the normal breast epithelial line, MCF-10 A. Cell types were chosen to identify hit compounds with specific toxicity towards either macrophages of a certain polarization state, cancer cells, or normal cells. Identifying leads with cell-line specific toxicity has major clinical implications. For example, selective macrophage depletion is a viable strategy for cancer treatment.[47] Cancer-cell specific compounds are also important for reducing side-effects and preventing toxicity in normal tissue.[48] Compounds were evaluated with or without light irradiation. Specifically, compounds **1**–**22** (10 μM) were incubated with all cell types for 1 h, then left in the dark or irradiated with blue light (λ_{irr}=460–470 nm, t_{irr}=20 min, 56 J/cm^2) and viability was assessed using the MTT assay 72 h after irradiation was ceased to identify photoactive PCT or PDT compounds.

Results of the screening experiment are shown in heat map form in Figure 2. Numerical data in Figure 2 are percent viabilities (vs. vehicle control as 100 %) from a single experiment but are representative of three independent experiments. Entries are color-coded in gradient form from orange to blue transitioning from low to high viabilities. Compounds **1**–**4** are a closely related series of dirhodium complexes with two formamidinate (form$^-$) bridging ligands and two neutral chelating ligands, which display potent toxicity toward both lines of polarized macrophages, with **1** and **2** displaying some amount of light activated toxicity. Compounds **1**–**3** display a lack of selectivity toward non-cancerous cells while **4** shows toxicity towards normal MCF-10 A cells. Therefore **1**–**3** were selected as candidates for EC_{50} determination. Compound **5** is also a Rh_2(II,II) complex bridged by two form$^-$ moieties that also possesses two additional neutral bridging ligands, which shows potent toxicity across all cell lines and was selected for further investigation.

Ruthenium compounds **6** and **7** bear the tridentate ligand dqpy and show rich structure-activity relationships. Ruthenium compound **6** is essentially non-toxic against all five cell lines, independent of light irradiation. Compound **7** bears an acetylacetonate (acac$^-$) ligand and was selected for further investigation; compounds of this type show favorable cellular toxicity properties and cancer cell selectivity.[49] Compound **8**, which is closely related to **7**, bearing a 2,2,6,6-tetramethyl-3,5-heptanedione (thd) ligand displayed potent toxicity across all cell lines and was also selected for further investigation. Compounds **9**–**19** all contain the $Ru(bpy)_2$ fragment, with two monodentate ligands or one bidentate ligand occupying the other coordination sites. Compound **11** is related to **7** and contains the acac$^-$ ligand, yet **11** displays no notable toxicity toward any of the cell lines. Compounds **12** and **9** likely suffer from poor cellular uptake as a result of bearing two bpy ligands, as evidenced by

their lack of activity. Furthermore, **9** is known to be an excellent photosensitizer,[50] yet is inactive in cells, likely due to its poor internalization. Compound **10** is closely related to **9**, bearing a deprotonated phenylpyridine ligand rather than bpy found in **19**, which reduces the overall charge of **10** to + 1. This reduction in charge results in greater lipophilicity in **10** vs. **9**, lending to better cellular penetration and therefore more potent toxicity. Compounds **13**–**15** bear anionic N-heterocyclic carbene (NHC^-) ligands, resulting in a reduction of charge by one unit compared to **9**. These compounds are closely related, varying only at the meta position on the pyridine ring of the NHC^- ligand, yet their properties are remarkably different. Both **13** and **14** show similarities in their toxicities toward polarized macrophage and towards the non-immune cell lines, yet **14** shows great potency toward non-polarized macrophages that **13** does not. Based on this finding, compound **14** was selected for further investigation. Comparatively, complex **15** bearing a nitro group was mostly inactive in the viability screen. Compounds **16**–**20** represent a panel of $Ru(bpy)_2$ containing complexes with a variety of triphenylphosphine (TPP) ligands. Compound **16** displays some capacity for light-induced toxicity, however **20**, a bisphen compound, improves upon the light-activated toxicity of **16**. Therefore, **20** was selected for future experimentation. Compounds **18** and **17** are mostly ineffective across all lines. Compound **19**, however displays potent light activated toxicity, specifically in macrophages, and was therefore selected for further investigation. Ruthenium compound **21** shows excellent light activated toxicity specifically toward M1 and M2 macrophages and was also selected for further study. Lastly, **22** is a well-known dual-action compound, capable of both photo-dissociation and photosensitization. Compound **22** displays potent light-activated killing among each macrophage line and in the cancer cell line, while displaying a lack of selectivity toward the non-cancerous MCF-10 A line. Therefore **22**, was selected for further investigation.

EC_{50} determination

After screening was complete, eleven compounds were selected for rigorous EC_{50} determinations against murine macrophages (M0, M1 and M2), MDA-MB-231 and MCF-10 A cells (Table 1). Cells were incubated with each compound (25–0.1 μM) for 1 h, media was aspirated and replenished, then cells were irradiated with blue light (λ_{irr} = 460–470 nm, t_{irr} = 20 min, 56 J/cm^2) or left in the dark for 20 min, and viabilities were determined by MTT assay 72 h later. A media aspiration step was incorporated before irradiation in these EC_{50} experiments to exclude false positives, compounds incapable of traversing the cell membrane that produce cell-permeable and cytotoxic photoproducts. Compounds **1** and **2** were largely inactive under these conditions. However, compound **3** was not toxic toward MCF-10 A at concentrations <25 μM, but it did display specificity towards polarized macrophages (M1 and M2) and MDA-MB-231 cells. Thus, **3** was considered a lead. Compound **5** killed MCF-10 A cells at lower concentrations than the other cell lines. Although **7** did not show evidence of light activation, it did show sub-micromolar EC_{50} values against all cell lines except the normal MCF-10 A line. Compound **8** displayed sub-micromolar EC_{50} values across all cell lines, independent of light irradiation, but was not specific. Each of the previously mentioned compounds displayed little to no light-enhanced toxicity, showing phototherapeutic indices (PI) ($\frac{Dark\ EC_{50}}{Light\ EC_{50}}$) values of 3 or less (Table S1 in Supporting Information). Compounds **19** and **20** were not active under these conditions

and showed EC_{50} values >25 μM. Consistent with a prior report which suggested **21** is not readily taken up by cells,[44b] compound **21** was not active in MDA-MB-231 and MCF-10 A cells. However, **21** showed excellent ability to kill macrophages in a light-activated fashion, especially M2 macrophages (light EC_{50} = 0.7 ± 0.2 μM, PI>36) (Table S1). Lastly, compound **22** showed light-induced toxicity across all cell lines, showing the least potency in MCF-10 A cells and the most potency in polarized macrophages. Compound **22** showed excellent PI values of >25, >100 and >45 in M0, M1, and M2 macrophages respectively, and a respectable PI value of 7.4 in MDA-MB-231 cells (Table S1), making **22** a prime candidate to carry over into 3D cell culture experiments.

3D cell viability assays

Compounds **1**, **3**, **21** and **22** showed favorable properties in 2D culture and were moved forward to 3D experiments. Unlike 2D monolayer culture, where in vivo features are not reproduced, 3D spheroids mimic solid tumors by including interaction with the extracellular matrix (ECM), cell polarity, and cell-to-cell contacts, thus providing a more accurate context in which to evaluate potential drug candidates.[52] Furthermore, incorporating tumor cells and macrophages into heterogeneous 3D spheroids mimics cytokine signaling between the two cell types that drives macrophage polarization to the M2 state, mimicking TAMs in solid tumors. Finally, TAMs have been shown to reduce the efficacy of some chemotherapeutics in the tumor microenvironment, leading to chemoresistance.[53] Doxorubicin is a commonly employed breast cancer chemotherapeutic agent associated with chemoresistance and cardiotoxicity. Drugs that synergize with doxorubicin have the potential to mitigate these effects by making doxorubicin active at lower doses. In the following experiments, doxorubicin was evaluated in combination with lead complexes to determine whether the effect of doxorubicin can be exacerbated upon cell-type specific depletion using a metal complex.

Tumor spheroids were established on cultrex by combining MDA-MB-231 cells and murine bone marrow derived macrophages (BMM). Cells were incubated for 72 h after seeding to allow for spheroid formation. After 72 h, cells were treated with each compound (25 μM) for 24 h before being rinsed, followed by light irradiation (λ_{irr}=460–470 nm, t_{irr}=20 min, 56 J/cm^2). Viability was determined after 72 h using the alamar blue fluorescence assay. Interestingly, compounds **1** and **21** displayed little to no capacity to reduce cell viability in the co-culture experiment at 25 μM concentration and were not selected for further experimentation, which disagreed with the data from 2D experiments. However, compounds **3** and **22** did show a cytotoxic effect, with data for **3** displaying similar potency under light and dark conditions and data for **22** indicating light-activated toxicity (Figure 3A). Importantly, compounds **3** and **22** (25 μM) reduced cell viability in combination with low, non-lethal concentrations of doxorubicin (Figure 3B). Spheroids treated with doxorubicin (1.25 μM) alone displayed nearly 100 % viability versus vehicle control spheroids (Figure 3B). However, the combination of 25 μM **3** and 1.25 μM doxorubicin decreased viability to ~ 50 % of the control, independent of light irradiation, indicating synergistic toxicity. Furthermore, compound **22** (25 μM) slightly reduced cell viability only when irradiated with light and showed a reduction in viability to about 50 % when cells were co-treated with 1.25 uM doxorubicin in combination with light. Interestingly, the results of the 2D

experiments determined that **3** was able to selectively kill cancer cells while **22** was more selective towards polarized macrophages, yet when used in combination with doxorubicin, a similar effect was observed for both compounds. With these promising results, **3** and **22** were selected for further examination by flow cytometry and fluorescence microscopy to accurately characterize effects on MDA-MB-231 cells vs. macrophages in the heterogeneous mixture and to probe macrophage polarization and immunogenic cell death.

Flow cytometry

For flow cytometry experiments, spheroids established over 72 h period were treated with **3** or **22** (25 μM), either alone or in combination with doxorubicin for 24 h. After 24 h, the treatment media was aspirated and replaced with vehicle. Where indicated (denoted as "Light"), spheroids were irradiated (λ_{irr}=460–470 nm, t_{irr}=20 min, 56 J/cm^2) or left in the dark and after 72 h cells were harvested, dissociated, and stained for flow cytometric analysis. Markers for polarized macrophages (M1: iNOS and M2: arginase 1), for immunogenic cell death (calreticulin), and a general viability dye were used. Initial results indicated that the macrophage population was almost entirely polarized to the M2 state in all conditions as indicated by the relatively high arginase signal and the relatively low iNOS levels (Figure 4A). This finding is consistent with the literature, which suggests that tumor cells polarize recruited macrophages toward the M2 phenotype. Interestingly, arginase signal was increased in samples dosed with doxorubicin, a finding also consistent with the literature suggesting tumor cells induce macrophage polarization to the M2 subtype as a mechanism of chemotherapy resistance.[54] Compound **3** alone did not significantly affect overall viability (Figure 4B, Figure S1A), consistent with the results of the 3D spheroid assay; however, contrary to the alamar blue assay, overall viability was not significantly decreased in samples treated with **3** in combination with doxorubicin. There was a clear effect on macrophage viability in the combination of **3** and doxorubicin (Figure 4C, Figure S1B) as well as a small but notable increase in tumor cell calreticulin expression (Figure 4D). Based on our results in Figure 3, where irradiation did not enhance compound 3's toxicity, we did not combine compound **3** with light irradiation for the flow cytometry experiments. In the dark, **22**+ doxorubicin showed an increase in the non-viable tumor cell population by nearly 20 % vs. the control (Figure 4B), whereas the results of previous experiments showed no evidence of toxicity for the combo in the dark. At the 72 h time point following irradiation, **22** either alone or in combination with doxorubicin showed highly effective killing, yielding low viable cell counts (1,969 viable tumor cells in 22 Light and 1,506 viable tumor cells in 22 Dox Light groups), although calreticulin was elevated in remaining detectable cells (Figure 4D, Figure S1C). Therefore, we repeated the experiment utilizing a 4 h incubation time post-irradiation rather than 72 h in an effort to capture the effect on cells prior to necrotic death and lysis over the 72 h time period.[32b] Compound **22** showed clear light-activated toxicity with or without doxorubicin (Figure S2A). While both conditions did display relatively equivalent levels of increase in the overall non-viable macrophage population (Figure S2B), arginase levels were muted in samples treated with the combination of **22** and doxorubicin vs. doxorubicin alone either with or without light (Figure 4E). This finding suggests that the combination with **22** reduces doxorubicin-induced M2 macrophages. Furthermore, treatment with **22**, doxorubicin and light also produced the largest observed tumor cell calreticulin signal among all conditions

(Figure 4F, Figure S2C), which is consistent with our 72 h treatment results (Figure 4D, Figure S1C), altogether suggesting this combination may have optimal M2 macrophage killing with immunogenic cell death induction.

Confocal imaging

Compound **22** was selected for further experimentation after the flow cytometry results showed that it was able to deplete macrophages selectively, decrease arginase levels (M2 macrophage marker), and increase calreticulin signals (ICD marker). Confocal microscopy was utilized to quantify the overall viability as well as the calreticulin levels. Spheroids were treated with **22** (25 μM) either alone or in combination with 1.25 μM doxorubicin for 24 h. After 24 h the treatment media was aspirated and replaced with vehicle. Spheroids were irradiated (λ_{irr}=460–470 nm, t_{irr}=20 min, 56 J/cm^2) or left in the dark and incubated for 4 h before imaging. Calcein AM staining of live cultures revealed that the combination of **22** and doxorubicin was lethal to cells that were irradiated when compared to all other conditions including **22** alone in the light (Figure 5A,B). Cell Tracker Orange labeling was used to distinguish calcein AM-positive macrophages from calcein AM-positive tumor cells (Figure 5C,D). Quantification of calcein fluorescence in these two cell populations revealed that the combination of **22** and doxorubicin was particularly effective in killing the macrophages. Calreticulin signal was measured next across all conditions to assess for indicators of ICD (Figure 6). The combination of **22** and doxorubicin under light conditions showed clear evidence of calreticulin translocation to the cell surface. In particular, the pericellular region at the tumor spheroid/ECM interface showed heavy staining for calreticulin (Figure 6A,B). Signals from calreticulin in this region were quantified in Figure 6C, which shows that the combination of **22**, doxorubicin and light produced the largest amount of extracellular calreticulin. Taking the alamar blue 3D viability data, flow cytometry, and imaging data together, it is clear that the combination of **22**, doxorubicin and light depletes immunosuppressive macrophages and tumor cells, and leads to the highest expression of calreticulin, a key signaling event in ICD. Although the detection of extracellular calreticulin shows great potential for achieving immunogenicity, further studies in immune competent animal models will be needed to prove that our compounds are immunogenic.

Prior knowledge concerning Ru and Rh metal complexes and their effects on macrophages is limited compared to other metal complexes. In particular, gold compounds have been studied for their immunogenic effects and effects on TAMs. Recent work with Au(III) complexes,[55] among others,[22c,56] exemplifies the utility of gold complexes towards TAMs. Unlike gold, rhodium and ruthenium complexes have yet to be tested on macrophages in settings that mimic the tumor microenvironment. Prior work with Ru compounds and macrophages is limited mainly to carbon monoxide releasing molecules (CORMs) where released CO, rather than Ru, is likely the active agent.[24b–d,g,i] Rh CORMs have also been assessed for their ability to affect macrophage polarization through modulation of NO signaling.[24f] Furthermore, in the pursuit of assessing their anti-leishmania activity, both Ru and Rh complexes have been shown to display toxicity against macrophages.[24a,h] These limited examples, which relate Ru and Rh complexes to macrophages, have not assessed compound activity in TAMs. In the present study, Ru

and Rh complexes showed macrophage toxicity in biomimetic 3D co-culture, the ability to sensitize tumor spheroids to chemotherapy, and to initiate signaling events consistent with ICD. This study clearly establishes a new role for Ru and Rh in targeting TAMs.

Conclusions

As our understanding of the complexity of the tumor microenvironment has improved with time it is becoming increasingly imperative that efficacy of any potential anti-cancer agents should be evaluated against multiple components of the tumor; chief among these being the macrophages, a critical cell type shown to play a major role in tumor survival and metastasis. This report aimed to assess the ability of mono- and di-nuclear rhodium and ruthenium complexes for their capacity to elicit a specific toxic response in macrophages, cancer cells, or healthy tissue. A panel of 22 previously synthesized and fully characterized metal complexes was used at a single concentration to assess for toxic effects across five cell types both in the presence and absence of light irradiation. A group of 11 compounds, which showed promising attributes in the general screen, were then used to perform EC_{50} determination across all cell lines. EC_{50} determination narrowed the field further for complexes which would be brought into 3D cell culture experiments. Tumor spheroids consisting of MDA-MB-231 breast cancer cells co-cultured with bone marrow derived murine macrophages were utilized for 3D experimentation in an effort to more closely resemble the true nature of the tumor microenvironment. It is well documented that macrophages render chemotherapy less effective at killing tumor tissue.[53] Therefore, tumor spheroids were treated with two complexes, **3** and **22**, in tandem with doxorubicin, a known chemotherapeutic. Both complexes were able to significantly reduce cancer viability as compared to doxorubicin alone, suggesting sensitization to treatment. Cell surface exposure of calreticulin, a known facilitator of ICD, was also increased upon treatment, suggesting the mechanism of killing may promote adaptive immune priming. In addition to tumor cell death, macrophages were found to be targeted, with a concomitant reduction in the M2 classifier arginase. Collectively, this approach may release immune suppression and support anti-tumor T cell activation. Future studies will evaluate this potential in immune competent animal models. In summation, this study makes a strong case for the utility of Ru and Rh anti-cancer complexes against TAMs and support their development into real-word therapies.

Supplementary Material

Refer to Web version on PubMed Central for supplementary material.

Acknowledgements

These studies were partially supported by the NSF (CHE-2102508 to C.T. and J.K.) and NIH (NCI R01 CA251394 to I.P.). J.K. and H.G. acknowledge Wayne State University (Rumble Fellow-ship to N.T.) and Detroit Medical Center Foundation Research Grant (H.G.). We thank the Microscopy, Imaging and Cytometry Resources Core (MICR) for assistance with confocal imaging and flow cytometry analyses. MICR is supported, in part, by NIH Center grant P30 CA22453 to the Karmanos Cancer Institute and R50 CA251068–01 to Dr. Moin, Wayne State University.

Data Availability Statement

The data that support the findings of this study are available from the corresponding author upon reasonable request.

References

[1]. Lichtnekert J, Kawakami T, Parks WC, Duffield JS, Curr. Opin. Pharmacol. 2013, 13, 555–564. [PubMed: 23747023]

[2]. Hansson GK, Engl N. J. Med. 2005, 352, 1685–1695.

[3] a). Mantovani A, Marchesi F, Malesci A, Laghi L, Allavena P, Nat. Rev. Clin. Oncol. 2017, 14, 399–416; [PubMed: 28117416] b)Cassetta L, Fragkogianni S, Sims AH, Swierczak A, Forrester LM, Zhang H, Soong DYH, Cotechini T, Anur P, Lin EY, Fidanza A, Lopez-Yrigoyen M, Millar MR, Urman A, Ai Z, Spellman PT, Hwang ES, Dixon J, Wiechmann L, Coussens LM, Smith HO, Pollard JW, Cancer Cell 2019, 35, 538–539. [PubMed: 30991022]

[4]. Sica A, Mantovani A, J. Clin. Invest. 2012, 122, 787–795. [PubMed: 22378047]

[5]. Latour YL, Gobert AP, Wilson KT, Amino Acids 2020, 52, 151–160. [PubMed: 31016375]

[6]. Houghton AN, Guevara-Patiño JA, J. Clin. Invest. 2004, 114, 468–471. [PubMed: 15314682]

[7]. Argyle D, Kitamura T, Front. Immunol. 2018, 9, 1–15. [PubMed: 29403488]

[8]. Zhao X, Qu Y Sun J, Wang J, Liu X, Wang F, Zhang H, Wang W, Ma X, Gao X, Zhang S, Oncotarget 2017, 8, 30576–30586. [PubMed: 28427165]

[9] a). Chen Y, Song Y, Du W, Gong L, Chang H, Zou Z, J. Biomed. Sci. 2019, 26, 78; [PubMed: 31629410] b)Zheng Y, Fang Y-C, Li J, Onco. Lett. 2019, 18, 5399–5407.

[10]. Herndon TM, Demko SG, Jiang X, He K, Gootenberg JE, Cohen MH, Keegan P, Pazdur R, Oncologist 2012, 17, 1323–1328. [PubMed: 23002124]

[11]. Buchbinder EI, Desai A, Am. J. Clin. Oncol. 2016, 39.

[12]. Barkal AA, Brewer RE, Markovic M, Kowarsky M, Barkal SA, Zaro BW, Krishnan V, Hatakeyama J, Dorigo O, Barkal LJ, Weissman IL, Nature 2019, 572, 392–396. [PubMed: 31367043]

[13]. Lyle DB, Breger JC, Baeva LF, Shallcross JC, Durfor CN, Wang NS, Langone JJ, J. Biomed. Mater. Res. 2008, 93A, 893–904.

[14] a). Qian Y, Qiao S, Dai Y, Xu G, Dai B, Lu L, Yu X, Luo Q, Zhang Z, ACS Nano 2017, 11, 9536–9549; [PubMed: 28858473] b)Kim H, Kim Y, Kim I-H, Kim K, Choi Y, Theranostics 2014, 4, 1–11.

[15]. Demidova TN, Hamblin MR, Int. J. Immunopathol. Pharmacol. 2004, 17, 117–126. [PubMed: 15171812]

[16] a). Gandioso A, Purkait K, Gasser G, Chimia 2021, 75, 845–855; [PubMed: 34728011] b)Chellan P, Sadler PJ, Chem. Eur. J. 2020, 26, 8676–8688; [PubMed: 32452579] c)Cole HD, Roque JA, Lifshits LM, Hodges R, Barrett PC, Havrylyuk D, Heidary D, Ramasamy E, Cameron CG, Glazer EC, McFarland SA, Photochem. Photobiol. Sci. 2022, 98, 73–84;d)Murray BS, Dyson PJ, Curr. Opin. Chem. Biol. 2020, 56, 28–34; [PubMed: 31812831] e)Thota S, Rodrigues DA, Crans DC, Barreiro EJ, J. Med. Chem. 2018, 61, 5805–5821; [PubMed: 29446940] f)Knoll JD, Turro C, Coord. Chem. Rev. 2015, 282–283, 110–126;g)Monro S, Colon KL, Yin H, Roque J III, Konda P, Gujar S, Thummel RP, Lilge L, Cameron CG, McFarland SA, Chem. Rev. 2019, 119, 797–828; [PubMed: 30295467] h)Hess J, Huang H, Kaiser A, Pierroz V, Blacque O, Chao H, Gasser G, Chem. Eur. J. 2017, 23, 9888–9869; [PubMed: 28509422] i)Chow MJ, Licona C, Pastorin G, Mellitzer G, Ang WH, Gaiddon C, Chem. Sci. 2016, 7, 4117–4124; [PubMed: 30155055] j)Lameijer LN, Ernst D, Hopkins SL, Meijer MS, Askes SHC, Le Dévédec SE, Bonnet S, Angew. Chem. Int. Ed. 2017, 56, 11549–11553; Angew. Chem. 2017, 129, 11707–11711.

[17] a). Aguirre JD, Angeles-Boza AM, Chouai A, Pellois J-P, Turro C, Dunbar KR, J. Am. Chem. Soc. 2009, 131, 11353–11360; [PubMed: 19624128] b)Truong D, Sullivan MP, Tong KKH, Steel TR, Prause A, Lovett JH, Andersen JW, Jamieson SMF, Harris HH, Ott I, Weekley CM,

Hummitzsch K, Söhnel T, Hanif M, Metzler-Nolte N, Goldstone DC, G Hartinger C, Inorg. Chem. 2020, 59, 3281–3289; [PubMed: 32073260] c)Graf M, Siegmund D, Metzler-Nolte N, Sünkel K, Böttcher H-C, Inorg. Chim. Acta 2019, 487, 9–14.

[18] a). Poynton FE, Bright SA, Blasco S, Williams DC, Kelly JM, Gunnlaugsson T, Chem. Soc. Rev. 2017, 46, 7706–7756; [PubMed: 29177281] b)White JK, Schmehl RH, Turro C, Inorg. Chim. Acta 2017, 454, 7–20;c)Heinemann F, Karges J, Gasser G, Acc. Chem. Res. 2017, 50, 2727–2736; [PubMed: 29058879] d)Bonnet S, Dalton Trans. 2018, 47, 10330–10343. [PubMed: 29978870]

[19]. Ghosh G, Colon KL, Fuller A, Sainuddin T, Bradner E, McCain J, Monro SMA, Yin H, Hetu MW, Cameron CG, McFarland SA, Inorg. Chem. 2018, 57, 7694–7712. [PubMed: 29927243]

[20] a). Erck A, Sherwood E, Bear JL, Kimbal AP, Cancer Res. 1976, 36, 2205–2209;b)Rao PN, Smith ML, Pathak S, Howard RA, Bear JL, Nat J. Cancer Institute. 1980, 64, 905–912.

[21]. Angeles-Boza AM, Bradley PM, Fu PK-L, Wicke SE, Bacsa J, Dunbar KR, Turro C, Inorg. Chem. 2004, 43, 8510–8519. [PubMed: 15606200]

[22] a). Lee SY, Kim CY, Nam T-G, Drug Des. Dev. Ther. 2020, 14, 5375–5392;b)Máliková K, Masaryk L, Štarha P, Inorganics 2021, 9, 26;c)Englinger B, Pirker C, Heffeter P, Terenzi A, Kowol CR, Keppler BK, Berger W, Chem. Rev. 2019, 119, 1519–1624; [PubMed: 30489072] d)Thota S, Rodrigues DA, Crans DC, Barreiro EJ, J. Med. Chem. 2018, 61, 5805–5821; [PubMed: 29446940] e)Popolin C, Cominetti MR, Med. Chem. 2017, 17, 1435–1441.

[23] a). Rausch M, Dyson PJ, Nowak-Sliwinska P, Adv. Ther. 2019, 2, 1900042.

[24] a). Costa MS, Concalves YG, Nunes DCO, Napolitano DR, Maia PIS, Rodrigues RS, Rodrigues VM, von Poelhsitz G, Yoneyama KAG, J. Inorg. Biochem. 2017, 175, 225–231; [PubMed: 28783554] b)Lee DW, Shin HY, Jeong JH, Han J, Ryu S, Nakahira K, Moon J-S, Biochem. Biophys. Res. Commun. 2017, 493, 957–963; [PubMed: 28942141] c)Yamamoto-Oka H, Mizuguchi S, Toda M, Minamiyama Y, Takemura S, Shibata T, Cepinskas G, Nishiyama N, Inflammopharmacology 2017, 26, 435–445; [PubMed: 28674739] d)Eun-Young Choi S-HC, Hyeon J-Y, Choi J-I, Choi S, Kim S-J, Eur. J. Pharmacol. 2015, 764, 22–29; [PubMed: 26101061] e)Liu SL-J, Lin S, Chan DS-J, Vong CT, Hoi PM, Wong C-Y, Ma D-L, Leung CH, J. Inorg. Biochem. 2014, 140, 23–28; [PubMed: 25046384] f)Moragues ME, Brines R, Terencio M, Sancenón F, Martínez-Máñez R, Alcaraz M, Inorg. Chem. 2013, 52, 13806–13808; [PubMed: 24279454] g)Sawle P, Foresti R, Mann BE, Johnson TR, Green CJ, Motterlini R, Br. J. Pharmacol. 2009, 145, 800–810;h)Rodriguez-Cabezas MN, Mesa-Valle CM, Azzouz S, Moraleda-Lindez V, Craciunescu D, Gutierrez-Rios MT, De Frutos MI, Osuna A, Pharmacol. 2001, 63, 112–119;i)Otterbein LE, Bach FH, Alam J, Soares M, Lu HT, Wysk M, Davis RJ, Flavell RA, Choi AMK, Nat. Med. 2000, 6, 422–428; [PubMed: 10742149] j)Aresta M, De Fazio M, Fumarulo R, Giordano D, Pantaleo R, Riccardi S, Biochem. Biophys. Res. Commun. 1982, 104, 121–125. [PubMed: 7073663]

[25]. White TA, Witt SE, Li Z, Dunbar KR, Turro C, Inorg. Chem. 2015, 54, 10042–10048. [PubMed: 26406159]

[26]. Li Z, Leed NA, Dickson-Karn NM, Dunbar KR, Turro C, Chem. Sci. 2014, 5, 727–737.

[27]. Turro C, Dunbar KR, " Multimetallic Systems for the Photocatalytic Production of Fuels from Abundant Sources", can be found under https://www.osti.gov/servlets/purl/1430648/, 2018.

[28]. Whittemore TJ, Xue C, Huang J, Gallucci JC, Turro C, Nat. Chem. 2020, 12, 180–185. [PubMed: 31959960]

[29]. Thummel R, Jahng Y, Inorg. Chem. 1986, 25, 2527–2534.

[30]. Al-Afyouni MH, Rohrabaugh TN, Al-Afyouni KF, Turro C, Chem. Sci. 2018, 9. 6711–6720. [PubMed: 30310605]

[31]. Loftus LM, Al-Afyouni KF, Turro C, Chem. Eur. J. 2018, 24, 11550–11553. [PubMed: 29923260]

[32] a). Toupin N, Steinke SJ, Nadella S, Li A, Rohrabaugh TN, Samuels ER, Turro C, Sevrioukova IF, Kodanko JJ, J. Am. Chem. Soc. 2021, 24, 9191–9205;b)Toupin NP, Nadella S, Steinke SJ, Turro C, Kodanko JJ, Inorg. Chem. 2020, 59, 3919–3933; [PubMed: 32096986] c)van Rixel VHS, Ramu V, Auyeung AB, Beztsinna N, Leger DY, Lameijer LN, Hilt ST, Le Dévédec SE, Yildiz T, Betancourt T, Gildner MB, Hudnall TW, Sol V, Liagre B, Kornienko A, Bonnet S, J. Am. Chem. Soc. 2019, 141, 18444–18454; [PubMed: 31625740] d)Arora K, Herroon M, Al-Afyouni MH,

Toupin NP, Rohrabaugh TN, Loftus LM, Podgorski I, Turro C, Kodanko JJ, J. Am. Chem. Soc. 2018, 140, 14367–14380; [PubMed: 30278123] e)Lameijer LN, Hopkins SL, Brevé TG, Askes SHC, Bonnet S, Chem. Eur. J. 2016, 22, 18484–18491. [PubMed: 27859843]

[33]. Bossmann SH, Turro C, Schnabel C, Pokhrel MR, Payawan LM, Baumeister B, Woerner M, J. Phys. Chem. B 2001, 105, 5374–5382.

[34]. Muro-Small ML, Yarnell JE, McCusker CE, Castellano FN, Eur. J. Inorg. Chem. 2012, 2012, 4004–4011.

[35]. Xiao X, Sakamoto J, Tanabe M, Yamazaki S, Yamabe S, Matsumura- Inoue T, J. Electroanal. Chem. 2002, 527, 33–40.

[36]. Garner RN, Joyce LE, Turro C, Inorg. Chem. 2011, 50, 4384–4391. [PubMed: 21504184]

[37]. Kender WT, Turro C, J. Phys. Chem. A 2019, 123, 2650–2660. [PubMed: 30896168]

[38] a). Respondek T, Sharma R, Herroon MK, Garner RN, Knoll JD, Cueny E, Turro C, Podgorski I, Kodanko JJ, ChemMedChem 2014, 9, 1306–1315; [PubMed: 24729544] b)Howerton BS, Heidary DK, Glazer EC, J. Am. Chem. Soc. 2012, 134, 8324–8327; [PubMed: 22553960] c)Respondek T, Garner RN, Herroon MK, Podgorski I, Turro C, Kodanko JJ, J. Am. Chem. Soc. 2011, 133, 17164–17167; [PubMed: 21973207] d)Byrne A, Burke CS, Keyes TE, Chem. Sci. 2016, 7, 6551–6562; [PubMed: 28042459] e)Zayat L, Salierno M, Etchenique R, Inorg. Chem. 2006, 45, 1728–1731. [PubMed: 16471986]

[39]. Litke SV, Ershov AY, Meyer TJ, J. Phys. Chem. A 2011, 115, 14235–14242. [PubMed: 22013947]

[40]. Marmion ME, Takeuchi KJ, J. Am. Chem. Soc. 1988, 110, 1472–1480.

[41]. Lanquist AP, Gupta S, Al-Afyouni KF, Al-Afyouni M, Kodanko JJ, Turro C, Chem. Sci. 2021, 12, 12056–12067. [PubMed: 34667571]

[42]. Huang EK, Cheung W, Chan SL, Sung HHY, Williams ID, Leung W, Organometallics 2013, 32, 4483–4489.

[43]. Liu Y, Hammett R, Lutterman DA, Joyce LE, Thummel R, Turro C, Inorg. Chem. 2009, 48, 375–385. [PubMed: 19035764]

[44] a). Liu Y, Hammitt R, Lutterman DA, Joyce LE, Thummel RP, Turro C, Inorg. Chem. 2009, 48, 375–385; [PubMed: 19035764] b)Zhao R, Hammitt R, Thummel RP, Liu Y, Turro C, Snapka RM, Dalton Trans. 2009, 251, 10926–10931;c)Sun Y, El Ojaimi M, Hammitt R, Thummel RP, Turro C, J. Phys. Chem. B 2010, 114, 14664–14670. [PubMed: 20545332]

[45]. Knoll JD, Albani BA, Turro C, Chem. Commun. 2015, 51, 8777–8780.

[46]. Knoll JD, Albani BA, Turro C, Acc. Chem. Res. 2015, 48, 2280–2287. [PubMed: 26186416]

[47]. Ries CH, Cannarile MA, Hoves S, Benz J, Wartha K, Runza V, Rey-Giraud F, Pradel LP, Feuerhake F, Klaman I, Jones T, Jucknischke U, Scheiblich S, Kaluza K, Gorr IH, Walz A, Abiraj K, Cassier PA, Sica A, Gomez-Roca C, de Visser KE, Italiano A, Le Tourneau C, Delord J, Levitsky H, Blay J, Ruttinger D, Cancer Cell 2014, 25, 846–859. [PubMed: 24898549]

[48]. Schirrmacher V, Int. J. Oncol. 2018, 54, 407–419. [PubMed: 30570109]

[49]. Gupta S, Vandevord JM, Loftus LM, Toupin N, Al-Afyouni MH, Rohrabaugh TN, Turro C, Kodanko JJ, Inorg. Chem. 2021, 60, 18964–18974. [PubMed: 34846875]

[50]. Demas JN, Harris EW, McBride RP, J. Am. Chem. Soc. 1977, 99, 3547–3551.

[51]. Toupin NP, Nadella S, Steinke SJ, Turro C, Kodanko JJ, Inorg. Chem. 2020, 59, 3919–3933. [PubMed: 32096986]

[52] a). Lovitt CJ, Shelper TB, Avery VM, Assay Drug Dev. Technol. 2013, 11, 435–448; [PubMed: 25310845] b)Elliott NT, Yuan F, J. Pharm. Sci. 2011, 100, 59–74. [PubMed: 20533556]

[53]. Shree T, Olson OC, Elie BT, Kester JC, Garfall AL, Simpson K, Bell-McGuinn KM, Zabor EC, Brogi E, Joyce JA, Genes Dev. 2011, 25, 2465–2479. [PubMed: 22156207]

[54]. Zhang Z, Sun C, Li C, Jiao X, Griffin BB, Dongol S, Wu H, Zhang C, Cao W, Dong R, Yang X, Zhang Q, Kong B, Front. Oncol. 2020, 10, 1.15.

[55]. Zhang J, Jiang M, Li S, Zhang Z, Sun H, Yang F, Liang H, J. Med. Chem. 2021, 64, 6777–6791. [PubMed: 34000198]

[56] a). Jurgens S, Casini A, Int. J. Chem. Sci. 2017, 71, 92–101;b)Zetterström CK, Jiang W, Wähämaa H, Östberg T, Aveberger A, Schierbeck H, Lotze MT, Andersson U, Pisetsky DS,

Harris HE, Leukocyte Biol J. 2008, 83, 31–38;c)Han S, Kim K, Kim H, Kwon J, Lee Y, Lee C, Song Y, Lee S, Ha N, Kim K, Arch. Pharmacal Res. 2008, 31, 67–74.

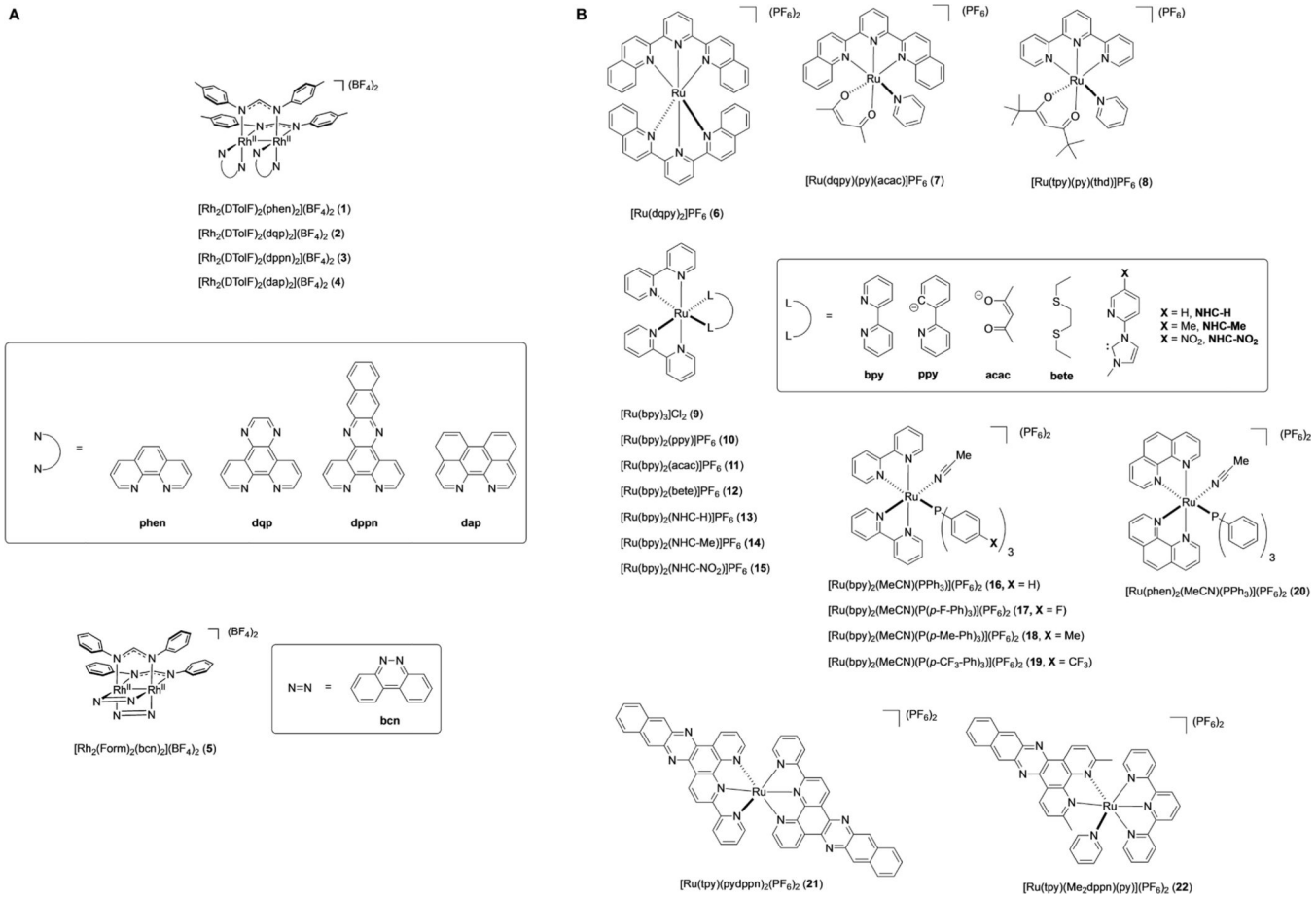

Figure 1.

Structures and formulas of dirhodium paddlewheel complexes **1**–**5** (A) and ruthenium complexes **6**–**22** (B).

#	M0		M1		M2		MDA		MCF	
	Light	Dark	Light	Dark	Light	Dark	Light	Dark	Light	Dark
1	100	86	9	53	8	26	25	65	86	84
2	100	92	9	19	13	36	84	80	95	90
3	59	38	7	4	2	3	0	39	82	99
4	91	86	6	2	3	4	55	29	24	19
5	2	2	8	6	5	2	4	32	6	44
6	100	100	45	29	50	51	70	73	81	99
7	2	5	10	4	3	2	2	6	2	10
8	5	3	4	4	4	1	4	4	4	1
9	94	92	86	84	45	99	100	92	85	91
10	2	2	0	11	0	0	1	4	11	37
11	92	94	95	91	100	100	32	32	28	38
12	96	79	100	94	100	89	95	88	82	88
13	81	86	3	13	4	24	18	19	39	44
14	1	1	0	1	0	0	19	16	43	44
15	75	98	21	36	79	65	28	31	36	39
16	73	100	31	87	56	101	8	75	24	73
17	100	100	100	91	77	96	32	93	47	83
18	100	100	81	93	66	100	77	97	40	100
19	17	100	2	41	7	62	33	85	35	55
20	28	100	10	60	22	86	6	75	27	47
21	4	100	11	88	14	92	63	74	40	56
22	1	100	9	97	0	84	6	96	35	98

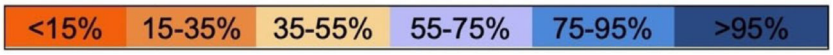

Figure 2.

Heat map for light and dark cell viabilities of 5 cell lines treated with compounds **1**–**22**. Cells were treated with compound **1**–**22** (10 μM) and either irradiated (λ_{irr}=460–470 nm, t_{irr}=20 min, 56 J/cm^2) or left in the dark. Cells were incubated for 72 h before viabilities were evaluated by MTT assay. Values in Figure 2 are represented as % viability vs. vehicle control with the same cell type. Values range from low viabilities (<15 %: bright orange) to high viability (>95 %: dark blue). Light alone did not decrease viability vs. non-irradiated controls. Viability data are averages from quadruplicate wells. Data are representative from three independent experiments. MDA: MDA-MB-231; MCF: MCF-10 A.

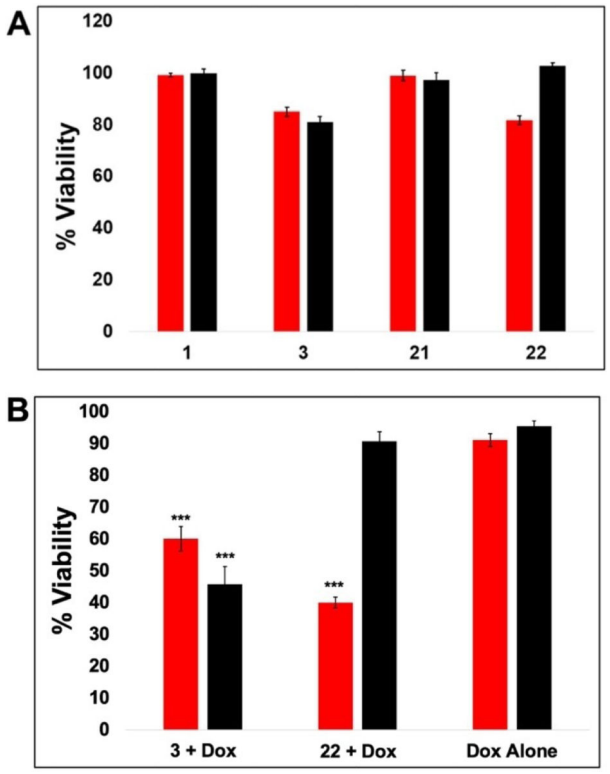

Figure 3.

Co-culture Macrophage/TNBC 3D Spheroids Viability Assays. **A**: 3D tumor spheroids treated with 25 μM **1**,**3**,**21**, or **22** for 24 h in the presence (**red**) or absence (**black**) of 20 min blue light (460/70 nm) irradiation. Viability was assessed by alamar blue assay 72 h after light treatment **B**: 3D tumor spheroids treated with 1.25 μM doxorubicin and either 25 μM **3**, **22**, or vehicle for 24 h in the presence (**red**) or absence (**black**) of 20 min blue light (460/70 nm) irradiation. Viability was assessed by alamar blue assay 72 h after light treatment. Statistical significance was determined against doxorubicin alone *** P <0.01.

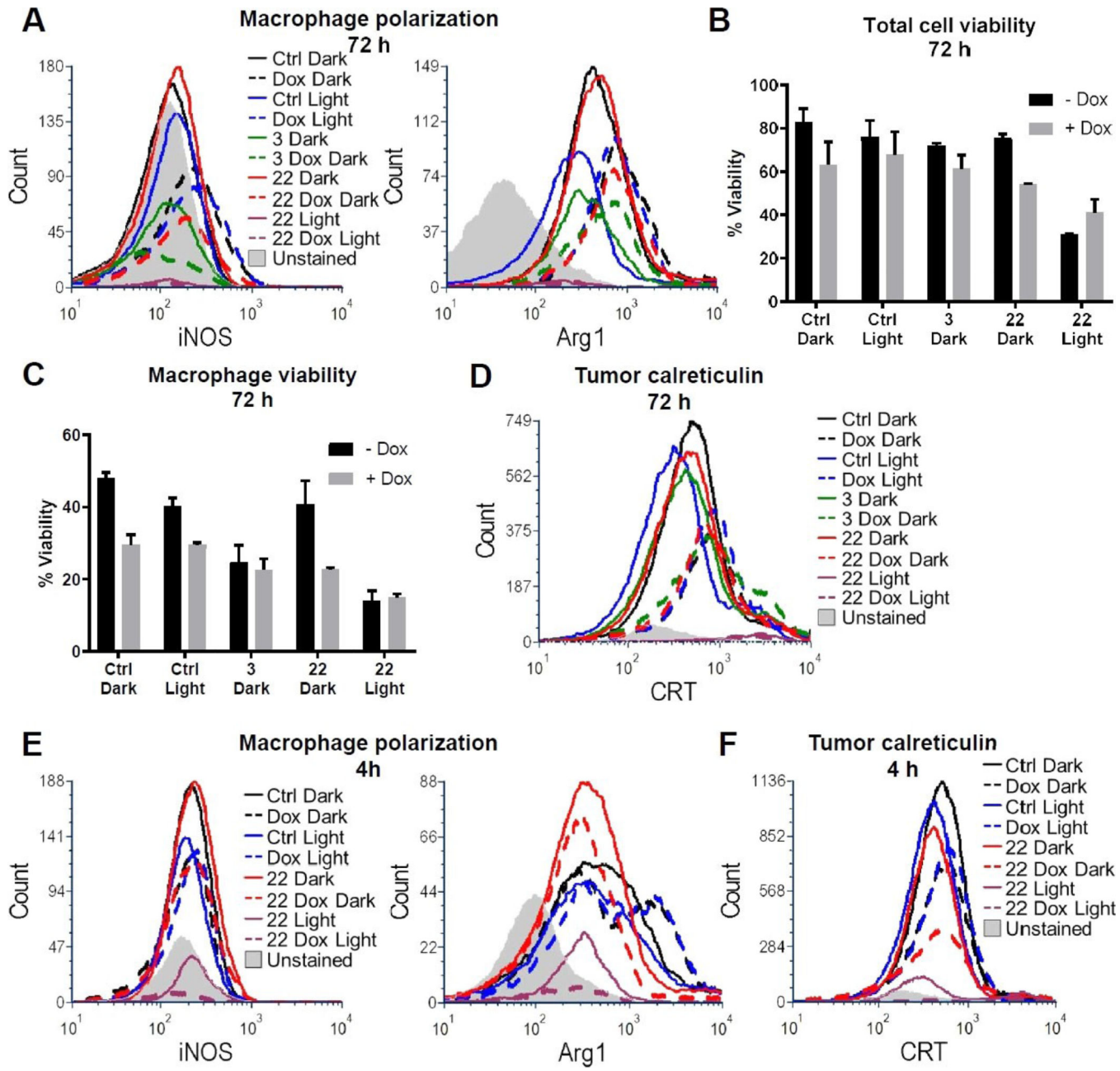

Figure 4.

Flow cytometry assessment of macrophage polarization and immunogenic cell death. 3D tumor spheroids were treated with vehicle, 25 μM **3** or **22** for 24 h, with or without 1.25 μM doxorubicin, with and without exposure to 20 min blue light (460/70 nm) irradiation as indicated. Spheroids were dissociated 72 h (**A**–**D**) or 4 h (**E**–**F**) after light treatment and stained for flow cytometric analysis. The unstained sample for all histograms is 3,000 unstained cells from the dissociated Ctrl Dark sample at the appropriate time point. **A**: Macrophage polarization after 72 h was determined by intracellular iNOS (M1) or Arg1 (M2) detection in F4/80 + macrophages. Viability was assessed after 72 h on the (**B**) total cell and (**C**) F4/80 + macrophage populations. Results are shown as the average +/− SD

from two independent biological replicates. **D**: Surface calreticulin exposure levels were detected on CD45-/F4/80-tumor cells 72 h after treatment. **E**: Macrophage polarization was assessed as in (**A**) 4 h after treatment. **F**: Tumor cell surface calreticulin exposure was assessed as in (**D**) 4 h after treatment.

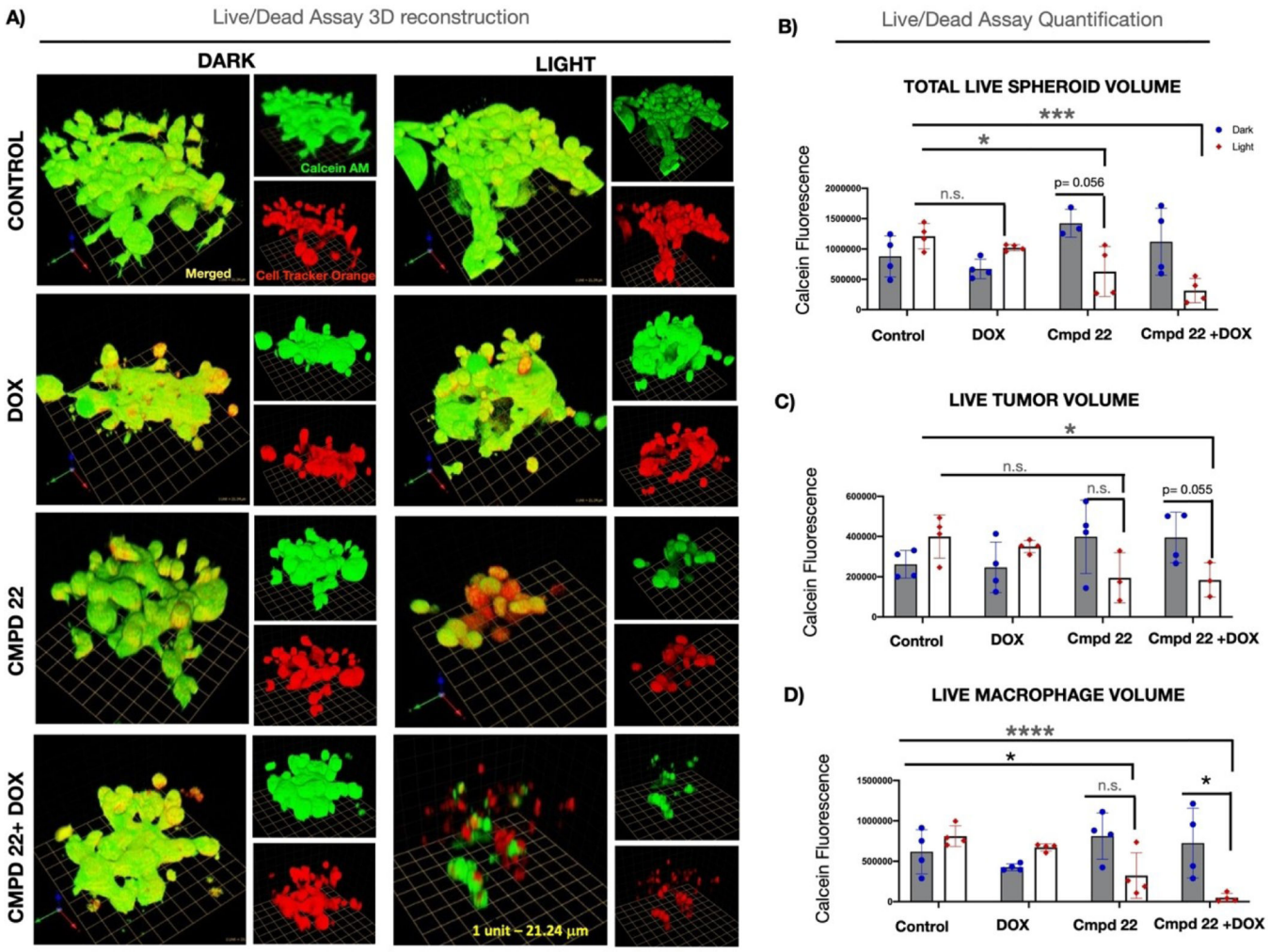

Figure 5.

Assessment of viability of 3D cultures exposed to **22** and Doxorubicin. **A**: 3D reconstruction of Calcein AM-stained 3D MDA MB 231/Macrophage spheroids treated with **22** (Cmpd **22**), doxorubicin (DOX) or combination of the two (Cmpd 2 + DOX); green: Calcein AM-positive live tumor cells; red: Cell Tracker Orange-labeled macrophages; yellow: live macrophages; merged 3D image and separate Calcein AM and Orange Tracker Red images are shown for each condition; 1 unit in the scale grid corresponds to 21.24 µm. **B**: Quantification of all Calcein AM-positive (live) cells in the spheroid [tumor cells (green) +macrophages(yellow)] shown as integrated fluorescence intensity; **C**: Quantification of live tumor cells (green) shown as integrated fluorescence intensity; **D**: Quantification of live macrophages (yellow) shown as integrated fluorescence intensity. Data are shown as individual values from at least 3 different spheroids/condition and are representative of 3 biological replicates. Statistical values were determined by student t-test. * $p<0.05$; ***$p<0.001$; ****$p<0.0001$; n.s. – not significant.

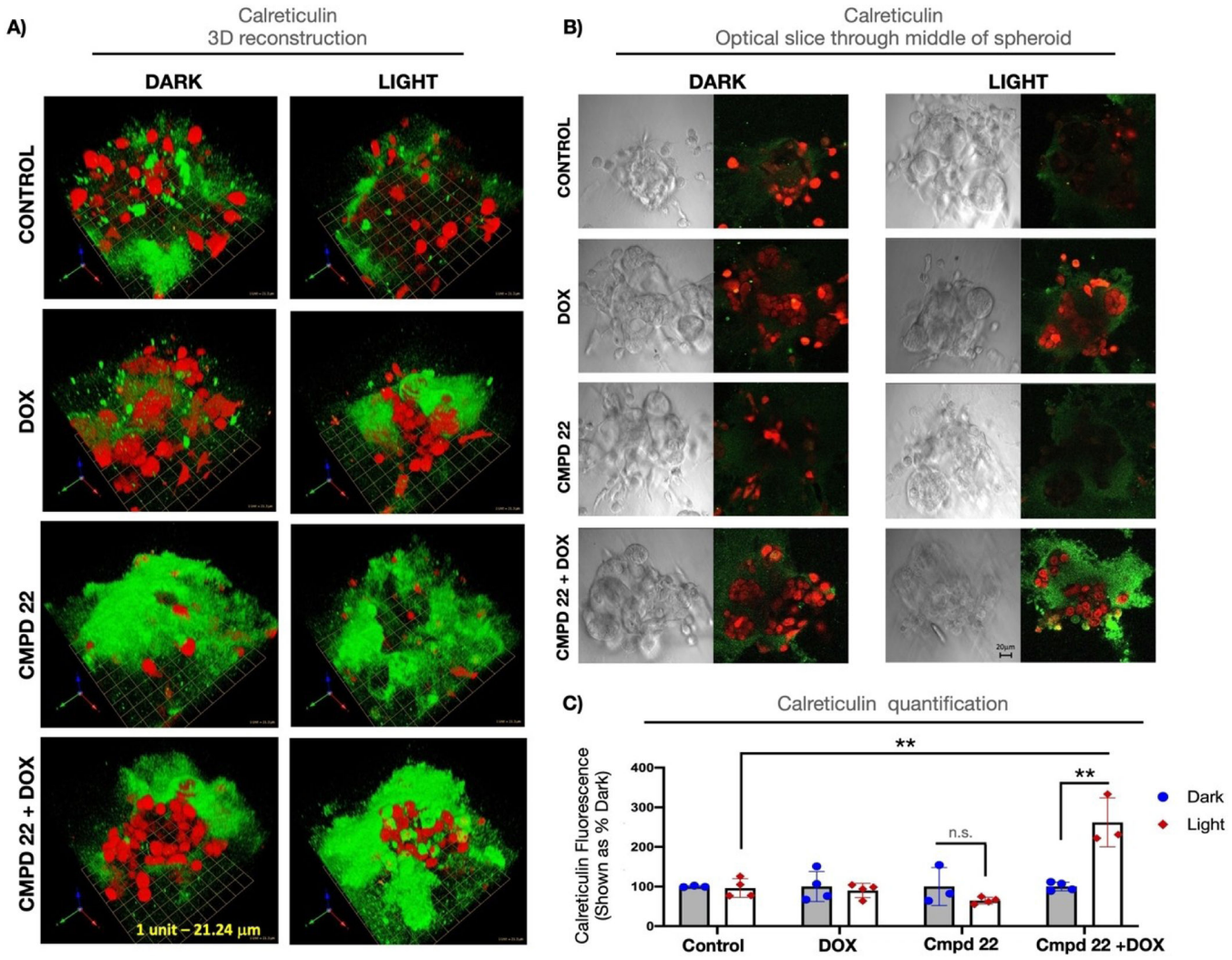

Figure 6.

Quantification of immunofluorescence staining for calreticulin in 3D tumor/macrophage spheroids. **A**: 3D reconstruction of Calreticulin staining (green) in 3D MDA MB 231/ Macrophage spheroids treated with **22** (Compound **22**), doxorubicin (DOX) or combination of the two (Compound **2** + DOX); red: Cell Tracker Orange-labeled macrophages; 1 unit in the scale grid corresponds to 21.24 µm. **B**: DIC (differential interference contrast) images of the middle slice (left panels) depicting morphology of the spheroids and middle slice depiction of calreticulin staining (right panels; green: calreticulin staining, red: Cell Tracker Orange-labeled macrophages); scale bar indicates 20 µm. **C**: Quantification of calreticulin staining shown as sum of surface fluorescence intensities throughout the Z-stack. Data are shown as calreticulin fluorescence in light-irradiated sample relative to its non-irradiated (dark) control. Individual values from at least 3 different spheroids/condition are depicted and are representative of 3 biological replicates. Statistical values were determined by student t-test. ** $p<0.01$; n.s. – not significant.

Table 1.

EC_{50} Values (μM) of Metal Complexes against Various Cell Lines.[a]

Entry	Compound	M0 Light	Dark	M1 Light	Dark	M2 Light	Dark	MDA-MB-231 Light	Dark	MCF-10A Light	Dark
1	**1**	22 ± 5	> 25	24 ± 1	> 25	20 ± 5	> 25	16 ± 5	15 ± 4	> 25	> 25
2	**2**	16 ± 3	> 25	12 ± 3	> 25	13 ± 1	> 25	> 25	> 25	> 25	> 25
3	**3**	20 ± 5	> 25	24 ± 1	15 ± 4	20 ± 4	24 ± 1.0	8.6 ± 2	9.3 ± 0.5	> 25	> 25
4	**5**	3.0 ± 2.1	3.4 ± 0.6	1.5 ± 0.9	1.8 ± 0.8	1.4 ± 0.7	3.0 ± 0.5	8.4 ± 1.1	8.4 ± 1.8	2.1 ± 1.2	2.9 ± 2.1
5	**7**	0.2 ± 0.04	0.3 ± 0.1	0.45 ± 0.2	0.99 ± 0.1	0.40 ± 0.11	1.7 ± 1.0	0.58 ± 0.07	0.67 ± 0.1	2.1 ± 1.1	1.7 ± 0.3
6	**8**	0.25 ± 0.14	0.75 ± 0.3	1.1 ± 0.1	0.89 ± 0.3	0.46 ± 0.2	0.88 ± 0.3	1.7 ± 0.7	2.8 ± 0.5	0.90 ± 0.2	1.2 ± 0.2
7	**14**	2.3 ± 1.9	1.7 ± 1.0	4.6 ± 1.2	13 ± 5	8.2 ± 2.6	17 ± 3	1.8 ± 0.8	1.4 ± 0.5	3.1 ± 0.4	7.8 ± 0.9
8	**19**	> 25	> 25	> 25	> 25	> 25	> 25	> 25	> 25	> 25	> 25
9	**20**	> 25	> 25	> 25	> 25	> 25	> 25	> 25	> 25	> 25	> 25
10	**21**	1.4 ± 0.4	> 25	2.2 ± 0.4	> 25	0.7 ± 0.2	> 25	> 25	> 25	> 25	> 25
11	**22**	1.0 ± 0.1	> 25	0.23 ± 0.14	> 25	0.55 ± 0.1	> 25	4.6 ± 0.5[b]	34 ± 3[b]	7.0 ± 2.1	> 25

[a]Cells of each type were exposed to experimental treatments in media ranging from 25 μM-100 nM for 1 h. Following treatment, media was aspirated and replaced with fresh media. Cells were then either irradiated with blue (460/70 nm) light for 20 min or wrapped in foil and incubated for 72 h before relative viabilities were determined by MTT assay. EC_{50} values were obtained using the Igor Pro graphing software. Data are averages of three independent experiments using quadruplicate wells, errors are standard deviations.

[b]Previously reported by Toupin et al.[51]